Diels–Alder Reaction on Free C68 Fullerene and Endohedral Sc3N@C68 Fullerene Violating the Isolated Pentagon Rule: Importance of Pentagon Adjacency

ARTICLE *in* CHEMISTRY - AN ASIAN JOURNAL · SEPTEMBER 2014

Impact Factor: 4.59 · DOI: 10.1002/asia.201402435

4 AUTHORS, INCLUDING:

Tao Yang
Shanghai Second Polytechnic University
26 PUBLICATIONS **228** CITATIONS
SEE PROFILE

Xiang Zhao
Xi'an Jiaotong University
130 PUBLICATIONS **1,274** CITATIONS
SEE PROFILE

CHEMISTRY
AN ASIAN JOURNAL
ACES
FULL PAPER

DOI: 10.1002/asia.201402435

Diels–Alder Reaction on Free C_{68} Fullerene and Endohedral $Sc_3N@C_{68}$ Fullerene Violating the Isolated Pentagon Rule: Importance of Pentagon Adjacency

Tao Yang,[a] Xiang Zhao,*[a] Shigeru Nagase,[b] and Takeshi Akasaka[c]

Abstract: The reaction mechanism and regioselectivity of the Diels–Alder reactions of C_{68} and $Sc_3N@C_{68}$, which violate the isolated pentagon rule, were studied with density functional theory calculations. For C_{68}, the [5,5] bond is the most favored thermodynamically, whereas the cycloaddition on the [5,6] bond has the lowest activation energy. Upon encapsulation of the metallic cluster, the exohedral reactivity of $Sc_3N@C_{68}$ is reduced remarkably owing to charge transfer from the cluster to the fullerene cage. The [5,5] bond becomes the most reactive site thermodynamically and kinetically. The bonds around the pentagon adjacency show the highest chemical reactivity, which demonstrates the importance of pentagon adjacency. Furthermore, the viability of Diels–Alder cycloadditions of several dienes and $Sc_3N@C_{68}$ was examined theoretically. *o*-Quinodimethane is predicted to react with $Sc_3N@C_{68}$ easily, which implies the possibility of using Diels–Alder cycloaddition to functionalize $Sc_3N@C_{68}$.

Keywords: cycloaddition · density functional calculations · fullerenes · reaction mechanisms · regioselectivity

Introduction

Trimetallic nitride template (TNT) endohedral fullerenes have attracted wide interest since they was first synthesized by Dorn et al. in 1999.[1] By encapsulating a M_3N cluster inside, the carbon cage formally accepts six electrons from the metallic cluster, which results in an electronic structure of $[M_3N]^{6+}@C_{2n}{}^{6-}$.[2] Charge transfer between the metallic cluster and the fullerene cage modifies the physical and chemical properties of endohedral fullerenes, and this significantly influences their chemical reactivity.[1,3] $Sc_3N@C_{68}$ is viewed as one of the most representative TNT endohedral fullerenes, not only because it is the smallest TNT endohedral fullerene found so far, but also because it is the first synthesized TNT endohedral fullerene that violates the well-known isolated pentagon rule (IPR).[4,5]

Chemical functionalization of endohedral fullerenes facilitates their structural characterization, tunes their physical and chemical properties, and expands their potential applications; thus, it has been a hot topic in fullerene science recently.[1,6] Diels–Alder (DA) reactions are commonly used to produce exohedral derivatives of endohedral fullerenes. Several endohedral fullerenes including $M_3N@C_{80}$ (M = Sc, Lu, and Gd) and $La@C_{82}$ have been revealed to undergo DA reactions.[7]

To understand exohedral reactivity for the DA reaction on endohedral fullerenes, Poblet and co-workers theoretically investigated some free and TNT endohedral fullerenes, including C_{2n} and $Sc_3N@C_{2n}$, ($2n = 68$, 78, and 80), and they predicted that the C–C bonds with a high Mayer bond order (MBO, corresponding to a short bond length) and high pyramidalization angles are the most reactive sites.[8] However, through studying the DA reaction of both endohedral (Sc_3N, Y_3N, and Ti_2C_2) and free C_{2n} ($2n = 78$ and 80) fullerenes, Solà et al. found that C–C bonds with long lengths also exhibit high reactivity.[9] Indeed, the reason why DA reactions take place on the long C–C bond of $Y_3N@C_{78}$ stems from the size of the metallic cluster inside.[9b] Notably, Solà and co-workers also selected several typical bonds in the IPR-violating free $C_2(22010)$–C_{78} and endohedral $M_3N@C_2(22010)$–C_{78} (M = Sc or Y) fullerenes and investigated energies for the DA reactions upon these C–C bonds (the nomenclature and symmetry of fullerene cages is specified by Fowler's spiral algorithm).[11] Their calculation results showed that the [5,5] bond is the most thermodynamically reactive site, not only for the free fullerene but also for endohedral fullerenes.

[a] Dr. T. Yang, Prof. Dr. X. Zhao
Institute for Chemical Physics & Department of Chemistry
Xi'an Jiaotong University
Xi'an 710049 (China)
Fax: (+86) 29-8266-8559
E-mail: xzhao@mail.xjtu.edu.cn

[b] Prof. Dr. S. Nagase
Fukui Institute for Fundamental Chemistry
Kyoto University
Kyoto 606-8103 (Japan)

[c] Prof. Dr. T. Akasaka
Department of Chemistry
Tokyo Gakugei University
Tokyo 184-8501 (Japan)

Supporting information for this article is available on the WWW under http://dx.doi.org/10.1002/asia.201402435.

Given that most of the above research has mainly focused on IPR-obeying fullerenes and endohedral fullerenes, systemic investigation of IPR-violating free and endohedral fullerenes is still lacking. Several essential questions remain open for DA reactions of IPR-violating endohedral fullerenes such as $Sc_3N@C_{68}$, which exhibit excellent physical and chemical properties. First, as the presence of pentagon adjacency introduces two new carbon bonds (types E and F in Figure 1) into the fullerene surface, do they show higher

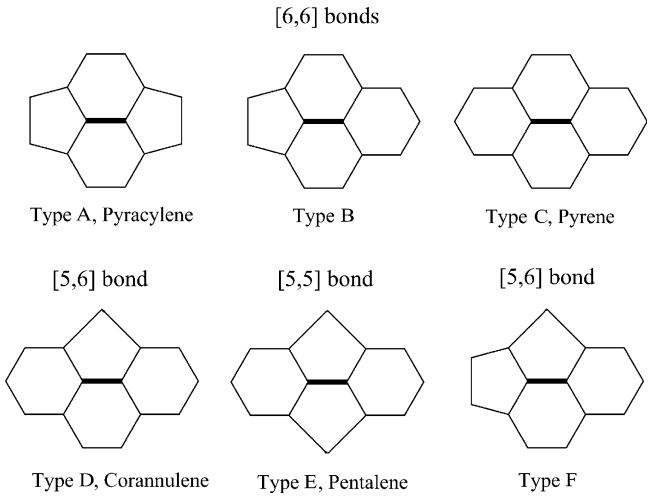

Figure 1. Representation of the different [6,6], [5,6], and [5,5] bond types presented in the fullerene structures, which were first proposed by Poblet and co-workers.[8]

or lower chemical reactivity than the other four C–C bonds? Second, the encapsulation of a TNT cluster changes the exohedral reactivity and regioselectivity of IPR fullerenes. Is the reactivity and regioselectivity of IPR-violating fullerenes also influenced by the TNT cluster? Third, considering the different chemical reactivity of dienes, which one can be chosen to functionalize non-IPR endohedral fullerene? Answers to the above questions will provide a comprehensive understanding of the DA chemistry of free and endohedral fullerenes and, more importantly, will help us to use DA reactions to chemically modify, purify, and functionalize non-IPR free and endohedral fullerenes.

In the present work, we performed a computational study of the mechanism of the DA reaction of free C_{68} fullerene and endohedral $Sc_3N@C_{68}$ fullerene by using density functional theory (DFT) calculations. To determine the most reactive sites and the changes in the exohedral reactivity induced by the metallic cluster, we first investigated both the thermodynamics and the kinetics of the DA reaction of 1,3-butadiene over all the nonequivalent bonds of C_{68} and $Sc_3N@C_{68}$. Then, the viability of DA reactions of several other dienes onto $Sc_3N@C_{68}$ was assessed theoretically to determine the best candidate for experimentalists to try and evaluate the effect of dienes on DA reactions.

Computational Methodology

All the DFT calculations were performed by using the Gaussian09[11] program. The exchange-correlation density functionals of Becke and Perdew (BP86)[12] were employed to optimize reactants and products and to locate transition states. The Lanl2dz[13] basis set with the corresponding effective core potential was used for Sc, and the 6-31G(d)[14] basis set was used for H, C, and N. Frequency calculations were performed to confirm all the reactants and products as local minima and all the transition states having one (and only one) imaginary frequency. Considering the large number of calculations, intrinsic reaction coordinate (IRC) calculations were only performed on several typical transition states to verify that those transition states did connect the reactants and products.[15] The reaction energies and barriers were corrected by zero-point energies derived from harmonic frequency calculations. To include the dispersion corrections, single-point energy calculations at the M06-2X[16]/Lanl2dz~6-31G(d) level of theory were performed on the optimized molecular structures at the BP86/Lanl2dz~6-31G(d) level [i.e., M06-2X/Lanl2dz~6-31G(d)//BP86/Lanl2dz~6-31G(d)]. Notably, the initial complexes were fully optimized at the M06-2X/Lanl2dz~6-31G(d) level.

Results and Discussion

DA Reactions of 1,3-butadiene with Free C_{68} Fullerene and Endohedral $Sc_3N@C_{68}$ Fullerene

$Sc_3N@C_{68}$ possesses the $D_3(6140)$–C_{68} cage.[4] As shown in Figure 2, the $D_3(6140)$–C_{68} fullerene has 18 nonequivalent C–C bonds that can be classified into the 6 types shown in Figure 1: pyracylenic or type A (bond a), type B (bonds b, c, d, e, f, and g), pyrenic or type C (bond h), corannulenic or type D (bonds i, j, k, l, m, n, and o), pentalenic or type E (bond p), and type E (bonds q and r). For $Sc_3N@C_{68}$, the Sc_3N cluster is not able to rotate within the cage around the C_3 axis owing to the relatively small size of the cage and the coordination between the Sc atoms and pentalene sites. The endohedral compound maintains its D_3 symmetry, and the

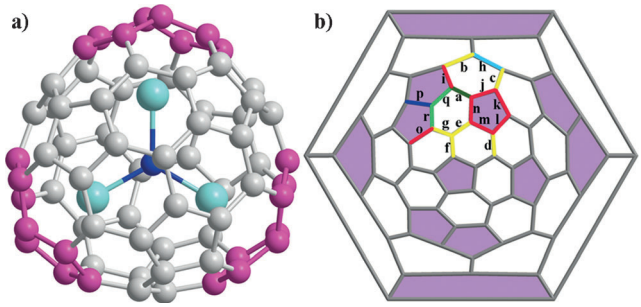

Figure 2. a) The molecular structure of $Sc_3N@D_3(6140)$-C_{68}, in which three pairs of pentagon adjacencies are colored deep red. b) The Schlegel diagram of the $D_3(6140)$-C_{68} fullerene cage, in which 18 nonequivalent bonds are marked with letters and highlighted by colors. The six different colors used define the six bond types.

number of nonequivalent C–C bonds does not change. Compared with IPR-obeying carbon cages, the $D_3(6140)$–C_{68} cage has two more C–C bond types, types E and F, as a consequence of pentagon adjacency. The reaction energies of 1,3-butadiene over all nonequivalent bonds of C_{68} and $Sc_3N@C_{68}$ are listed in Table 1.

Table 1. The predicted reaction energies (ΔE_r) and energy barriers ($\Delta E^{\neq}$) for the DA reaction of 1,3-butadiene over all 18 nonequivalent bonds in free C_{68} fullerene and endohedral $Sc_3N@C_{68}$ fullerene at the BP86/Lanl2dz~6-31G(d) level of theory.

Bond	Bond type	C_{68}		$Sc_3N@C_{68}$	
		ΔE_r [kcal mol^{-1}]	$\Delta E^{\neq}$ [kcal mol^{-1}]	ΔE_r [kcal mol^{-1}]	$\Delta E^{\neq}$ [kcal mol^{-1}]
a	A[6,6]	−13.5	13.4	0.0	23.0
b	B[6,6]	−7.5	14.6	9.0	29.5
c	B[6,6]	−7.1	12.3	−3.0	22.8
d	B[6,6]	−0.5	12.9	8.2	30.0
e	B[6,6]	−5.6	12.7	3.9	25.4
f	B[6,6]	−2.8	15.9	4.4	28.7
g	B[6,6]	2.0	12.4	4.2	23.8
h	C[6,6]	20.0	31.3	−4.5	22.3
i	D[5,6]	−11.8	14.8	−5.7	20.9
j	D[5,6]	−13.9	13.4	−7.2	23.5
k	D[5,6]	−15.6	11.6	−4.5	22.2
l	D[5,6]	−12.1	13.6	−2.7	24.5
m	D[5,6]	−23.1	12.0	−5.4	22.4
n	D[5,6]	−13.9	13.6	−3.7	23.0
o	D[5,6]	−23.0	11.2	−3.2	22.0
p	E[5,5]	−39.8	7.9	−18.6	17.9
q	F[5,6]	−31.1	7.1	−10.1	19.3
r	F[5,6]	−23.7	8.1	−6.9	21.6

It is evident from Table 1 that the reaction energies are not always exothermic for the C–C bonds in the free fullerene and that they fall over a wide range from −39.8 to +20.0 kcal mol^{-1}. The most exothermic reaction was found for type E bond p (−39.8 kcal mol^{-1}) followed by type F bond q (−31.1 kcal mol^{-1}), whereas the least exothermic reaction was obtained for bond h (20.0 kcal mol^{-1}). There is a clear relationship between the bond types in the free fullerene and the corresponding reaction energies for DA reactions upon them. For the above six types of bonds, the predicted reaction energies mainly follow the order type C < type B < type A < type D < type F < type E. It was demonstrated by Solà and co-workers that the reaction energies of C_{78} fullerene also coincide with the above trend.[9]

The reason why the reaction energies mainly follow such an order stems from the strain energy induced by the pentagonal ring. Owing to the pentagonal ring, the reaction energy for the [5,6] bond is exothermic in the range from −11 to −31 kcal mol^{-1}. The high reactivity of type E bond p can be ascribed to the fact that the cycloaddition of 1,3-butadiene on the type E bond releases the high strain energy resulting from the two adjacent pentagons. In contrast, the most reactive bond among all the [6,6] bonds is type A bond a with a reaction energy of −13.5 kcal mol^{-1}, which coincides with previous results in C_{60} and C_{78}.[9]

If the TNT cluster is inside C_{68}, the reaction energies of all the nonequivalent C–C bonds in the resulting endohedral fullerene reduce dramatically and fall in a narrow range from −19 to +9 kcal mol^{-1}, which suggests that the DA reaction on the endohedral fullerene is less regioselective than that on the free fullerene, and this is analogous to free C_{78} and endohedral $Sc_3N@C_{78}$ fullerenes.[9a] In general, the encapsulation of the TNT cluster induces two opposite effects on the exohedral reactivity of the endohedral fullerenes.[9a] The geometric deformation caused by the TNT cluster enhances the strain energy, which gives rise to an increase in the exohedral reactivity, whereas charge transfer from the TNT cluster to the fullerene reduces the electron affinity and lowers the chemical reactivity. For $Sc_3N@C_{68}$, it seems that the charge transfer plays a much more important role than the geometric deformation; thus, the majority of the C–C bonds are noticeably deactivated in the endohedral fullerene. Indeed, the geometric deformation energy is predicted to be only 18.2 kcal mol^{-1}.

Solà and co-workers revealed recently that the exohedral reactivity of charged C_{60} fullerene is reduced remarkably if the number of electrons of C_{60} rises, which indicates that charge transfer has a significant influence on the exohedral reactivity of fullerenes.[17] Furthermore, by performing a thorough theoretical study of the DA reactivity of C_{80} (I_h)-based endohedral fullerenes, the same group found that endohedral fullerenes are less reactive than hollow C_{80} (I_h) cages, especially those with high charge transfer from the encapsulated metallic atoms or cluster to the fullerene cage.[18] Therefore, the amount of charge transferred to the fullerene cage would be the key factor in controlling the exohedral reactivity of the endohedral fullerenes.

The three most exothermic bonds of $Sc_3N@C_{68}$ are bonds p, q, and j with reaction energies of −18.6, −10.1, and −7.2 kcal mol^{-1}, respectively, but they are significantly destabilized by approximately 17–21 kcal mol^{-1}. The predicted reactivity trend for the bonds mainly follows the above order in the free fullerene, whereas only the chemical reactivity of type C bond h changes in the opposite direction. Indeed, bond h, which is endothermic in the free fullerene, is stabilized by approximately 24 kcal mol^{-1}, and it becomes exothermic with a reaction energy of −4.5 kcal mol^{-1}. On the basis of the calculations on several selected bonds, Solà and co-workers also found that the [5,5] bond in free $C_2(22010)$–C_{78} and endohedral $M_3N@C_2(22010)$–C_{78} (M = Sc or Y) fullerenes is the most exothermic bond.[9b]

To understand the kinetics of the above DA reactions, the concerted transition states (TSs) of the cycloaddition reactions for all the nonequivalent bonds in the free and endohedral fullerenes were located. Searching TS structures always starts from a symmetric structure, which means that the bond lengths of the two C–C bonds to be formed are the same; however, in most cases, it finally leads to an asynchronic TS. Noteworthy, asynchronic TSs are commonly found in DA reactions on fullerenes and endohedral fullerenes such as $M_3N@C_{78}$ (M = Sc, Y) and $M_3N@C_{80}$ (M = Sc, Lu, and Gd).[9,18]

The predicted energy barriers are collected in Table 1. It is clear that for the free fullerene, the three most exothermic products (resulting from bonds p, r, and q) still have the lowest energy barriers, but they are in a different order. The lowest barrier (7.1 kcal mol^{-1}) is found for the second most exothermic product (i.e., bond q), whereas the most exothermic product (i.e., bond p) shows the second lowest barrier of 7.9 kcal mol^{-1}. As a result, the product resulting from bond q is the kinetic product, whereas the product resulting from bond p is the thermodynamic product, and this suggests that the thermodynamic and kinetic products do not always correspond to the same adduct, which is also observed in the experiments of the 1,3-dipolar cycloaddition over $Sc_3N@C_{80}$, the Bingel–Hirsch reaction on $Sc_3N@C_{68}$, and the DA reaction over C_{78}.[6c,d,9a] The transition state and product of the DA cycloaddition of 1,3-butadiene and bond p of free C_{68} fullerene are shown in Figure 3.[19] Bond h, which is the most endothermic site, has the highest energy barrier in the free fullerene.

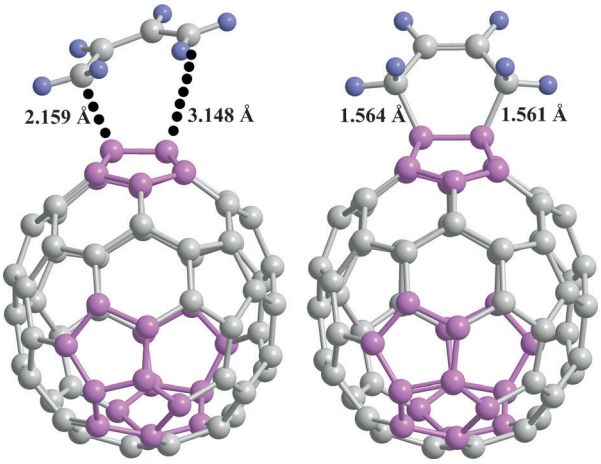

Figure 3. The optimized geometries of the transition state (left) and product (right) of 1,3-butadiene with type E bond p of free C_{68} fullerene. The three pairs of pentagon adjacencies in the fullerene cage are colored pink.

For the endohedral compound, the energy barriers are mostly higher with respect to the corresponding energy barriers in the free fullerene, which coincides with the above thermodynamic results. Therefore, from both thermodynamic and kinetic points of view, the encapsulation of the TNT cluster reduces the exohedral reactivity of the fullerene surface. Type E bond p with the most exothermic reaction energy also has the lowest energy barrier of 17.9 kcal mol^{-1}, which is close to that of the DA reaction between butadiene and ethylene or $Sc_3N@C_{78}$.[9a] The formation of the product from bond p for the DA reaction between $Sc_3N@C_{68}$ and 1,3-butadiene is favored thermodynamically and kinetically; this suggests that bond p, rather than the previously predicted [5,6] corannulene or type D bond l,[8] is the most reactive site.

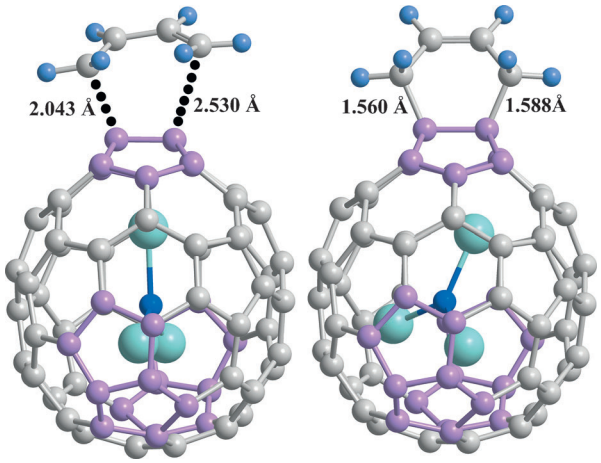

Figure 4. The optimized geometries of the transition state (left) and product (right) of 1,3-butadiene with type E bond p of endohedral $Sc_3N@C_{68}$ fullerene. The three pairs of pentagon adjacencies in the fullerene cage are colored pink.

Figure 4 depicts the transition state and product of the DA cycloaddition of 1,3-butadiene and bond p of endohedral $Sc_3N@C_{68}$ fullerene. The second and third lowest energy barriers are observed for reactions upon bond q (19.3 kcal mol^{-1}) and bond i (20.9 kcal mol^{-1}). Indeed, bond i is the fifth most exothermic bond. Similar to the thermodynamic results, only bond h has a lower energy barrier, which reduces from 31.3 kcal mol^{-1} in the free fullerene to 22.3 kcal mol^{-1} in the endohedral fullerene. Recently, Poblet and co-workers studied the Bingel–Hirsch addition upon $Sc_3N@C_{68}$ and disclosed that the product from bond i was under thermodynamic control, whereas the product from bond d was under kinetic control, as proposed from NMR experiments.[6d] As a consequence, the exohedral reactivity order of the C–C bonds on the fullerene surface depends strongly on the type of chemical reaction.

The Role of Bond Length, Pyramidalization Angle, and the Unoccupied Molecular Orbitals on Chemical Reactivity for Nonequivalent Bonds

The bond lengths and the pyramidalization angles are revealed to be effective predictors to deduce the chemical reactivity of the C–C bonds in fullerene cages; that is, C–C bonds with short bond lengths and high pyramidalization angles should be favored in cycloaddition reactions such as the DA reaction, because these bonds not only exhibit more double-bond character, but they also need less energy to deform to the transition states and this lowers the energy barriers.[9] To profoundly investigate the relationship between these physical predictors and chemical reactivity, the pyramidalization angles and bond lengths for all nonequivalent bonds are collected in Table 2.

Generally, the bond distance cannot be used to predict the chemical reactivity sequence of both the free and endohedral fullerenes very well. For the free fullerene, even

Table 2. Bond lengths (R_{cc}) and pyramidalization angles (θ_p) for all the nonequivalent bonds in free C_{68} fullerene and endohedral $Sc_3N@C_{68}$ fullerene.

Bond	Bond type	C_{68}		$Sc_3N@C_{68}$	
		R_{cc} [Å]	θ_p[a] [°]	R_{cc} [Å]	θ_p[a] [°]
a	A[6,6]	1.402	11.48	1.423	11.55
b	B[6,6]	1.426	9.91	1.460	9.59
c	B[6,6]	1.436	9.69	1.444	9.99
d	B[6,6]	1.437	9.53	1.438	9.54
e	B[6,6]	1.441	10.52	1.450	9.75
f	B[6,6]	1.422	9.71	1.436	9.41
g	B[6,6]	1.449	10.28	1.451	10.61
h	C[6,6]	1.492	8.62	1.469	9.07
i	D[5,6]	1.466	11.77	1.458	11.40
j	D[5,6]	1.447	10.68	1.442	10.64
k	D[5,6]	1.446	10.48	1.456	9.07
l	D[5,6]	1.457	10.05	1.446	10.34
m	D[5,6]	1.438	10.86	1.445	10.69
n	D[5,6]	1.455	11.77	1.455	10.63
o	D[5,6]	1.455	11.27	1.472	11.33
p	E[5,5]	1.439	16.18	1.452	16.55
q	F[5,6]	1.430	14.26	1.452	14.61
r	F[5,6]	1.433	13.76	1.461	14.54

[a] Average of the two pyramidalization angles of the carbon atoms involved.

though bonds a, b, and f possess the shortest bond lengths ranging from 1.402 to 1.422 Å, they provide modest exothermic products. Nevertheless, the reaction energies and the activation energies predict that bonds p, q, and r are the most reactive bonds, which are longer in length than bonds a, b, and f. Upon encapsulation of the TNT cluster, most of the C–C bonds become markedly enlarged, especially those bonds around the pentagon adjacency, as they are quite close to the endohedral metal atoms. However, the bond lengths of some type C and type D bonds including bonds h, i, and j become shorter in the endohedral fullerene. For the endohedral fullerene, the predicted order based on the bond length still does not agree well with the chemical reactivity trend. For example, bonds a, d, and f show the shortest bond lengths, whereas bonds i, j, p, and q exhibit the highest reactivity.

Relative to the bond length, the pyramidalization angle is a much better predictor. In the case of the free fullerene, bonds p, q, and r show the largest angles and are the most reactive bonds on the basis of the reaction and activation energies, even though they are in a different order. Likewise, the large endothermicity of bond h ($+20$ kcal mol^{-1}) concurs well with its low angle of 8.62°. Bond g has a considerable angle of 10.28°, which is even a little larger than that of bond l (10.05°), whereas bond g provides a considerably more endothermic product compared with the clear exothermicity of bond l. In the endohedral fullerene, bond p still has the largest angle, which is predicted to be the most reactive site. Bond q, with the largest angle of 14.61°, shows the second most exothermic reaction of 10.1 kcal mol^{-1}. Interestingly, bond r is similarly pyramidalized with bond p, but it is only modestly exothermic.

The molecular orbitals of the reactants, both the free and endohedral fullerenes, were also introduced to explain the chemical reactivity of the C–C bonds. It is well known that in DA reactions of fullerenes, the main orbital interaction takes place between the highest occupied molecular orbital (HOMO) of butadiene and the lowest unoccupied molecular orbitals (LUMOs) of the fullerene. The chemical reactivity is significantly influenced by the energy difference between the HOMO of butadiene (-5.62 eV) and the LUMOs of the fullerene; that is, the smaller the $LUMOs_{fullerene}$–$HOMO_{butadiene}$ gap, the higher the reactivity of the fullerene.

For the free fullerene, the energy levels of the LUMOs range from -4.72 to -2.27 eV. As a result of the charge transfer from the TNT cluster to the fullerene, the endohedral fullerene has much higher LUMOs from -3.59 to -3.07 eV, which results in lower reactivity toward butadiene compared with the free fullerene, and this concurs well with the above-calculated results. More importantly, according to the Woodward–Hoffmann rule[20] and frontier orbital theory,[21] only C–C bonds with the opposite sign and large contributions of the LUMOs would exhibit high reactivity in the DA cycloaddition reaction. As depicted in Figure 5, several bonds of C_{68}, including bonds a, b, e, f, k, m, o, p, q, and r, have suitable orbitals to interact with the HOMO of butadiene, but bonds p, q, and r show the highest chemical reactivity. In $Sc_3N@C_{68}$, the large contributions of the LUMO come from bonds a, k, and g; however, these bonds provide only modestly exothermic products. Bond p as the most reactive bond only has suitable orbitals in LUMO+2 and LUMO+3 with small contribution, which demonstrates that predictions based on LUMOs would not provide good results.

Compared with bond length and molecular orbitals, the pyramidalization angle supplies a better prediction for C_{68} and $Sc_3N@C_{68}$. The reason may be that in both non-IPR C_{68} and $Sc_3N@C_{68}$, the presence of the pentagon adjacency induces high local strain energy, which is reflected in the large pyramidalization angles around the pentagon adjacency. The cycloaddition reactions on the bonds around the pentagon adjacency will strongly release the local strain energy, which makes these bonds the most exothermic. Thus, the pyramidalization angle, rather than the bond length and molecular orbitals, plays a key role in determining the chemical reactivity of the C–C bonds in C_{68} and $Sc_3N@C_{68}$. It reasonable to deduce that the pyramidalization angle can also be viewed as a useful predictor for other fullerene cages with pentagon adjacency.

DA Reactions of a Series of Dienes on Endohedral $Sc_3N@C_{68}$ Fullerene

The DA reactions of several other dienes, including 1,3-cyclohexadiene, *o*-quinodimethane, and anthracene (Scheme 1), on endohedral $Sc_3N@C_{68}$ fullerene were investigated theoretically to disclose the role of the dienes. Dispersion corrections were considered, as it has been revealed that theoretical calculations including dispersion corrections

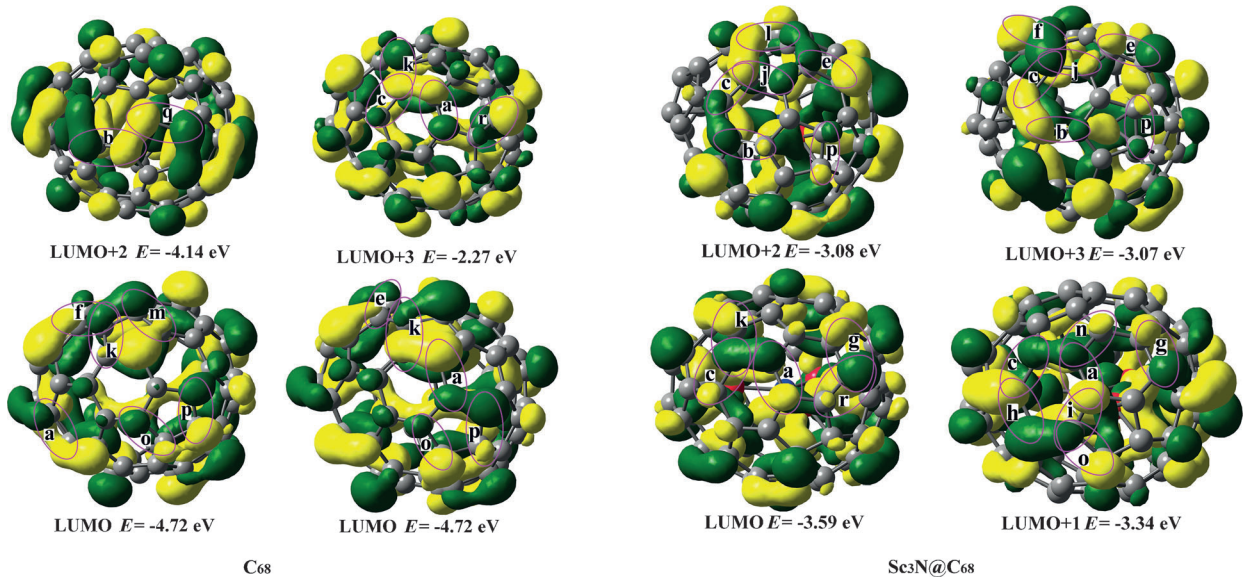

Figure 5. Representation of the low-lying unoccupied molecular orbitals of free C_{68} fullerene (right) and endohedral $Sc_3N@C_{68}$ fullerene (left). Only those bonds with favorable orbitals to interact with the HOMO of the diene are highlighted with ellipses.

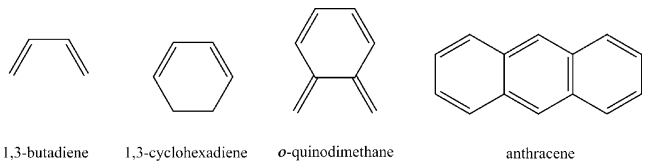

Scheme 1. Four dienes (1,3-butadiene, 1,3-cyclohexadiene, *o*-quinodimethane, and anthracene) selected for DA reactions on endohedral $Sc_3N@C_{68}$ fullerene.

provide more accurate results close to the experimental values.[7g,9c,22] Noteworthy, if the dispersion corrections are taken into consideration, an initial complex forms as a consequence of London dispersion interactions (Figure 6), and this results in stabilization of the reactants. Such initial complexes have also been found in theoretical studies of the DA

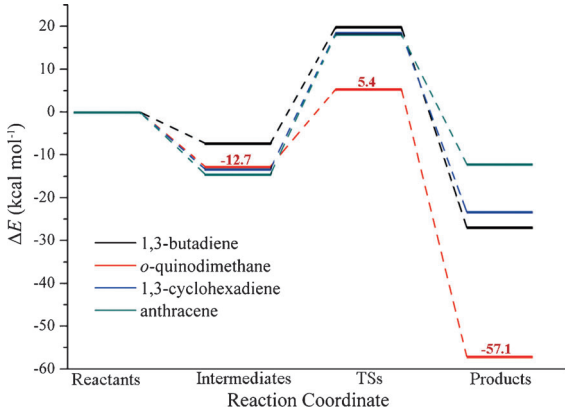

Figure 6. Energy profiles of the DA cycloadditions between four dienes (1,3-butadiene, *o*-quinodimethane, 1,3-cyclohexadiene, and anthracene) and endohedral $Sc_3N@C_{68}$ fullerene.

reaction upon the free and endohedral fullerenes such as $Ti_2C_2@C_{78}$ and $La@C_{82}$.[7g,h,9c] As mentioned above, the type E bond p is the most reactive site in $Sc_3N@C_{68}$. Hence, DA reactions of these dienes were investigated on the pentalenic bond, as shown in Table 3.

Table 3. The predicted energies of initial complexes (ΔE_{int}), energy barriers ($\Delta E^{\neq}$), and reaction energies (ΔE_r) for the DA reactions of the selected dienes on endohedral $Sc_3N@C_{68}$ fullerene at the M06-2X/Lanl2dz~6-31G(d)//BP86/Lanl2dz~6-31G(d) level of theory.

Diene	E_{HOMO} [eV]	ΔE_{int} [kcal mol^{-1}]	$\Delta E^{\neq}$ [kcal mol^{-1}]	$\Delta E_{int}^{\neq}$[a] [kcal mol^{-1}]	ΔE_r [kcal mol^{-1}]
1,3-butadiene	−5.62	−7.3	19.9	27.2	−26.9
o-quinodimethane	−4.58	−12.7	5.4	18.1	−57.1
1,3-cyclohexadiene	−4.86	−11.0	18.5	29.5	−23.3
anthracene	−4.73	−13.2	18.2	31.4	−12.1

[a] $\Delta E_{int}^{\neq}$ represents the barrier height by using the formed initial complex ΔE_{int} as a reference.

The predicted barrier and reaction energy of the DA reaction of 1,3-butadiene upon $Sc_3N@C_{68}$ were corrected to be 19.9 and −26.9 kcal mol^{-1}, respectively, owing to the inclusion of dispersion corrections. In view of the initial complex with the energy of −7.3 kcal mol^{-1}, the real barrier height is 27.2 kcal mol^{-1}, which indicates that the reaction would not be viable at room temperature.

The reaction of *o*-quinodimethane is quite exothermic by −57.1 kcal mol^{-1} with an energy barrier of only 5.4 kcal mol^{-1}. The barrier height is 18.1 kcal mol^{-1}, even though the initial complex was taken into account, as depicted in Figure 6. This clearly demonstrates that this reaction is experimentally feasible, and consequently, it is possible to use

DA cycloaddition chemistry to purify and functionalize $Sc_3N@C_{68}$. *o*-Quinodimethane is more reactive than 1,3-butadiene in DA reactions, and this may be due to the strong aromatic stabilization at the transition states and products.[23] The introduction of an electron-donating group into *o*-quinodimethane would increase its nucleophilicity and make the reaction more feasible. Indeed, the experimental DA reaction of endohedral fullerenes was firstly realized between 6,7-dimethoxyisochroman-3-one and $Sc_3N@C_{80}$.[7a]

Finally, the reaction energies of 1,3-cyclohexadiene and anthracene are predicted to be −23.3 and −12.1 kcal mol^{-1}, respectively. However, the high barriers from initial complexes to transition states, 29.5 and 31.4 kcal mol^{-1} for 1,3-cyclohexadiene and anthracene, respectively, suggest that these reactions are implausible.

The reactivity order of the four dienes can be well understood in terms of frontier orbital theory. The smaller the energy gap between the LUMO of the endohedral fullerene (−3.59 eV) and the HOMO of diene, the more easily the DA reaction. As showed in Table 3, the energy level of the LUMO of *o*-quinodimethane is the highest (−4.58 eV), which coincides with the fact that it is the most reactive diene.

Conclusions

With density functional theory calculations, we performed a systemic theoretical study of the thermodynamics and kinetics of the DA reactions of free C_{68} fullerene and endohedral $Sc_3N@C_{68}$ fullerene that violate the isolated pentagon rule. For the free fullerene, the product under thermodynamic control is obtained for cycloaddition to the [5,5] bond p, whereas under kinetic control, it corresponds to the type F bond q. Upon encapsulation of the TNT cluster, the exohedral reactivity of the endohedral fullerene is reduced remarkably owing to charge transfer from the cluster to the fullerene cage. Bond p is found to be the most reactive site thermodynamically and kinetically, which implies that the C−C bonds around the pentagon adjacency show the highest chemical reactivity. Compared with bond lengths and molecular orbitals, the pyramidalization angle is a more useful predictor for reactivity trend of the C−C bonds in C_{68} and $Sc_3N@C_{68}$. Our findings reveal that the presence of the pentagon adjacency leads to a significant change in the exohedral reactivity of the fullerene surfaces, which demonstrates the important role of the pentagon adjacency on the exohedral reactivity of free and endohedral fullerenes.

The DA cycloadditions of several dienes and $Sc_3N@C_{68}$ were also investigated theoretically. *o*-Quinodimethane was found to be the best candidate for experimentalists to purify and functionalize $Sc_3N@C_{68}$. Our work may not only shed light on the exohedral reactivity of non-IPR endohedral fullerenes, but it may also encourage further investigations of chemical reactions of free fullerenes and endohedral fullerenes.

Acknowledgements

This work was financially supported by the National Natural Science Foundation of China (21171138, 20673081), the National Key Basic Research Program of China (2011CB209404, 2012CB720904), and the Specialized Research Fund for the Doctoral Program of Higher Education of China (SRFDP No. 20130201110033).

[1] a) S. Stevenson, G. Rice, T. Glass, K. Harich, F. Cromer, M. R. Jordan, J. Craft, E. Hadju, R. Bible, M. M. Olmstead, K. Maitra, A. J. Fisher, A. L. Balch, H. C. Dorn, *Nature* **1999**, *401*, 55; b) H. Shinohara, *Rep. Prog. Phys.* **2000**, *63*, 843; c) *Endofullerenes: A New Family of Carbon Clusters* (Eds.: T. Akasaka, S. Nagase), Kluwer, Dordrecht, **2002**; d) N. Martín, *Chem. Commun.* **2006**, 2093; e) L. Dunsch, S. Yang, *Small* **2007**, *3*, 1298; f) M. N. Chaur, F. Melin, A. L. Ortiz, L. Echegoyen, *Angew. Chem. Int. Ed.* **2009**, *48*, 7514; *Angew. Chem.* **2009**, *121*, 7650; g) Y.-Z. Tan, S.-Y. Xie, R.-B. Huang, L.-S. Zheng, *Nat. Chem.* **2009**, *1*, 450; h) *Chemistry of Nanocarbons* (Eds.: T. Akasaka, F. Wudl, S. Nagase), Wiley, New York, **2010**; i) N. Martín, *Angew. Chem. Int. Ed.* **2011**, *50*, 5431; *Angew. Chem.* **2011**, *123*, 5543; j) A. Rodríguez-Fortea, A. L. Balch, J. M. Poblet, *Chem. Soc. Rev.* **2011**, *40*, 3551; k) X. Lu, T. Akasaka, S. Nagase, *Chem. Commun.* **2011**, *47*, 5942; l) S. Yang, F. Liu, C. Chen, M. Jiao, T. Wei, *Chem. Commun.* **2011**, *47*, 11822; m) X. Lu, L. Feng, T. Akasaka, S. Nagase, *Chem. Soc. Rev.* **2012**, *41*, 7723; n) J. Zhang, S. Stevenson, H. C. Dorn, *Acc. Chem. Res.* **2013**, *46*, 1548; o) A. A. Popov, S. Yang, L. Dunsch, *Chem. Rev.* **2013**, *113*, 5989; p) M. Garcia-Borràs, S. Osuna, M. Swart, J. M. Luis, M. Solà, *Chem. Soc. Rev.* **2014**, 43, 5089.

[2] a) J. M. Campanera, C. Bo, J. M. Poblet, *Angew. Chem. Int. Ed.* **2005**, *44*, 7230; *Angew. Chem.* **2005**, *117*, 7396; b) A. A. Popov, L. Dunsch, *J. Am. Chem. Soc.* **2007**, *129*, 11835; c) A. Rodríguez-Fortea, N. Alegret, A. L. Balch, J. M. Poblet, *Nat. Chem.* **2010**, *2*, 955; d) J. J. Zheng, X. Zhao, J. S. Dang, Y. M. Chen, Q. Xu, W. W. Wang, *Chem. Phys. Lett.* **2011**, *514*, 104; e) T. Yang, X. Zhao, L.-S. Li, J.-J. Zheng, W.-Y. Gao, *ChemPhysChem* **2012**, *13*, 449.

[3] a) S. Guha, K. Nakamoto, *Coord. Chem. Rev.* **2005**, *249*, 1111; b) Y. Iiduka, O. Ikenaga, A. Sakuraba, T. Wakahara, T. Tsuchiya, Y. Maeda, T. Nakahodo, T. Akasaka, M. Kako, N. Mizorogi, S. Nagase, *J. Am. Chem. Soc.* **2005**, *127*, 9956.

[4] a) S. Stevenson, P. W. Fowler, T. Heine, J. C. Duchamp, G. Rice, T. Glass, K. Harich, E. Hajdu, R. Bible, H. C. Dorn, *Nature* **2000**, *408*, 427; b) M. M. Olmstead, H. M. Lee, J. C. Duchamp, S. Stevenson, D. Marciu, H. C. Dorn, A. L. Balch, *Angew. Chem. Int. Ed.* **2003**, *42*, 900; *Angew. Chem.* **2003**, *115*, 928; c) S. Yang, M. Kalbac, A. Popov, L. Dunsch, *Chem. Eur. J.* **2006**, *12*, 7856.

[5] H. W. Kroto, *Nature* **1987**, *329*, 529.

[6] a) M. Yamada, T. Akasaka, S. Nagase, *Acc. Chem. Res.* **2010**, *43*, 92; b) S. Osuna, M. Swart, M. Solá, *Phys. Chem. Chem. Phys.* **2011**, *13*, 3585; c) A. Rodríguez-Fortea, J. M. Campanera, C. M. Cardona, L. Echegoyen, J. M. Poblet, *Angew. Chem. Int. Ed.* **2006**, *45*, 8176; *Angew. Chem.* **2006**, *118*, 8356; d) N. Alegret, A. Rodríguez-Fortea, J. M. Poblet, *Chem. Eur. J.* **2013**, *19*, 5061.

[7] a) E. B. Iezzi, J. C. Duchamp, K. Harich, T. E. Glass, H. M. Lee, M. M. Olmstead, A. L. Balch, H. C. Dorn, *J. Am. Chem. Soc.* **2002**, *124*, 524; b) H. M. Lee, M. M. Olmstead, E. Iezzi, J. C. Duchamp, H. C. Dorn, A. L. Balch, *J. Am. Chem. Soc.* **2002**, *124*, 3494; c) S. Stevenson, R. R. Stephen, T. M. Amos, V. R. Cadorette, J. E. Reid, J. P. Phillips, *J. Am. Chem. Soc.* **2005**, *127*, 12776; d) T. Cai, L. Xu, M. R. Anderson, Z. Ge, T. Zuo, X. Wang, M. M. Olmstead, A. L. Balch, H. W. Gibson, H. C. Dorn, *J. Am. Chem. Soc.* **2006**, *128*, 8581; e) Y. Maeda, J. Miyashita, T. Hasegawa, T. Wakahara, T. Tsuchiya, T. Nakahodo, T. Akasaka, N. Mizorogi, K. Kobayashi, S. Nagase, T. Kato, N. Ban, H. Nakajima, Y. Watanabe, *J. Am. Chem. Soc.* **2005**, *127*, 12190; f) Y. Maeda, S. Sato, K. Inada, H. Nikawa, M. Yamada, N. Mizorogi, T. Hasegawa, T. Tsuchiya, T. Akasaka, T. Kato, Z. Slanina, S. Nagase, *Chem. Eur. J.* **2010**, *16*, 2193; g) S. Sato, Y. Maeda, J.-D. Guo, M. Yamada, N. Mizorogi, S. Nagase, T. Akasa-

ka, *J. Am. Chem. Soc.* **2013**, *135*, 5582; h) M. Garcia-Borràs, J. M. Luis, M. Swart, M. Solà, *Chem. Eur. J.* **2013**, *19*, 4468.
[8] J. M. Campanera, C. Bo, J. M. Poblet, *J. Org. Chem.* **2006**, *71*, 46.
[9] a) S. Osuna, M. Swart, J. M. Campanera, J. M. Poblet, M. Solà, *J. Am. Chem. Soc.* **2008**, *130*, 6206; b) S. Osuna, M. Swart, M. Solà, *J. Am. Chem. Soc.* **2009**, *131*, 129; c) M. Garcia-Borràs, S. Osuna, J. M. Luis, M. Swart, M. Solà, *Chem. Eur. J.* **2012**, *18*, 7141; d) S. Osuna, R. Valencia, A. Rodríguez-Fortea, M. Swart, M. Solà, J. M. Poblet, *Chem. Eur. J.* **2012**, *18*, 8944.
[10] P. W. Fowler, D. E. Manolopoulos, *An Atlas of Fullerenes*, Clarendon Press, Oxford, **1995**.
[11] Gaussian 09, Revision A.01, M. J. Frisch, G. W. Trucks, H. B. Schlegel, G. E. Scuseria, M. A. Robb, J. R. Cheeseman, G. Scalmani, V. Barone, B. Mennucci, G. A. Petersson, H. Nakatsuji, M. Caricato, X. Li, H. P. Hratchian, A. F. Izmaylov, J. Bloino, G. Zheng, J. L. Sonnenberg, M. Hada, M. Ehara, K. Toyota, R. Fukuda, J. Hasegawa, M. Ishida, T. Nakajima, Y. Honda, O. Kitao, H. Nakai, T. Vreven, J. A. Montgomery, Jr., J. E. Peralta, F. Ogliaro, M. Bearpark, J. J. Heyd, E. Brothers, K. N. Kudin, V. N. Staroverov, R. Kobayashi, J. Normand, K. Raghavachari, A. Rendell, J. C. Burant, S. S. Iyengar, J. Tomasi, M. Cossi, N. Rega, J. M. Millam, M. Klene, J. E. Knox, J. B. Cross, V. Bakken, C. Adamo, J. Jaramillo, R. Gomperts, R. E. Stratmann, O. Yazyev, A. J. Austin, R. Cammi, C. Pomelli, J. W. Ochterski, R. L. Martin, K. Morokuma, V. G. Zakrzewski, G. A. Voth, P. Salvador, J. J. Dannenberg, S. Dapprich, A. D. Daniels, Ö. Farkas, J. B. Foresman, J. V. Ortiz, J. Cioslowski, D. J. Fox, Gaussian, Inc., Wallingford, CT, **2009**.
[12] a) A. D. Becke, *Phys. Rev. A* **1988**, *38*, 3098; b) J. P. Perdew, *Phys. Rev. B* **1986**, *33*, 8822.
[13] P. J. Hay, W. R. Wadt, *J. Chem. Phys.* **1985**, *82*, 299.
[14] a) P. C. Hariharan, J. A. Pople, *Theor. Chim. Acta* **1973**, *28*, 213; b) W. J. Hehre, R. Ditchfield, J. A. Pople, *J. Chem. Phys.* **1972**, *56*, 2257.
[15] a) K. Fukui, *J. Phys. Chem.* **1970**, *74*, 4161; b) C. Gonzalez, H. B. Schlegel, *J. Chem. Phys.* **1989**, *90*, 2154; c) C. Gonzalez, H. B. Schlegel, *J. Phys. Chem.* **1990**, *94*, 5523.
[16] Y. Zhao, D. Truhlar, *Theor. Chem. Acc.* **2008**, *120*, 215.
[17] a) M. Garcia-Borràs, S. Osuna, M. Swart, J. M. Luis, M. Solà, *Chem. Commun.* **2013**, *49*, 1220; b) I. Fernández, M. Solà, F. M. Bickelhaupt, *Chem. Eur. J.* **2013**, *19*, 7416.
[18] M. Garcia-Borràs, S. Osuna, J. M. Luis, M. Swart, M. Solà, *Chem. Eur. J.* **2013**, *19*, 14931.
[19] Given that this concerted TS structure is very asymmetric, we performed further calculations to confirm that it was the real one. First, the IRC calculation was performed on the TS structure, and the results showed that it connects the reactants and product. Second, the diradical and stepwise pathways were also investigated. The first step of both the diradical pathway and the stepwise pathway, which is the formation of the singlet diradical intermediate or triplet intermediate, is the rate-determining step. For the stepwise pathway, the energy barrier is 12.1 kcal mol^{-1}, which is higher than that of the concerted TS (7.9 kcal mol^{-1}). However, optimization of the singlet diradical TS always leads to the closed-shell singlet TS structure, which is indeed the concerted TS mentioned above, and this implies that the diradical pathway may not exist. Besides, the IRC calculation on TS of DA reaction over bond q, which also has a low energy barrier, was also performed to verify that it leads to the corresponding product. For details, see the Supporting Information.
[20] R. B. Woodward, R. Hoffmann, *Angew. Chem. Int. Ed. Engl.* **1969**, *8*, 781; *Angew. Chem.* **1969**, *81*, 797.
[21] K. Fukui, *Molecular Orbitals in Chemistry, Physics and Biology* (Eds.: P. O. Lowdin, B. Pullman), Academic Press, New York, **1964**, p. 513.
[22] a) R. S. Paton, J. L. Mackey, W. H. Kim, J. H. Lee, S. J. Danishefsky, K. N. Houk, *J. Am. Chem. Soc.* **2010**, *132*, 9335; b) S. Osuna, M. Swart, M. Solà, *J. Phys. Chem. A* **2011**, *115*, 3491.
[23] a) I. Klundt, *Chem. Rev.* **1970**, *70*, 471; b) M. Manoharan, P. Venuvanalingam, *J. Phys. Org. Chem.* **1998**, *11*, 133; c) M. Manoharan, F. De Proft, P. Goerlings, *J. Chem. Soc. Perkin Trans. 2* **2000**, 1767; d) M. Manoharan, F. De Proft, P. Geerlings, *J. Org. Chem.* **2000**, *65*, 7971.

Received: April 25, 2014
Published online: July 13, 2014